

https://doi.org/10.1070/QEL17478

Light–current characteristics of high-power pulsed semiconductor lasers (1060 nm) operating at increased (up to 90 °C) temperatures

P.S. Gavrina, A.A. Podoskin, E.V. Fomin, D.A. Veselov, V.V. Shamakhov, S.O. Slipchenko, N.A. Pikhtin, P.S. Kop'ev

Abstract. **Pulsed radiative characteristics of high-power semiconductor lasers based on an asymmetric InGaAs/AlGaAs/GaAs heterostructure with an active region including two quantum wells and a gradient waveguide on the side of the p-emitter are studied. It is shown that the use of the proposed design allows efficient laser operation under pumping by 100-ns current pulses in the temperature range 25–90 °C. The lasers with a Fabry–Perot cavity 2900 μm long demonstrated peak powers of 62 W (injection current 123 A) and 43 W (122 A) at temperatures of 25 and 90 °C, respectively. It is found that at room temperature and currents of ~50A, a decrease in the cavity length to 600 μm does not cause a decrease in the output power with respect to the power of lasers with a long (2900 μm) cavity. An increase in temperature to 90 °C at high injection currents leads to a sharp decrease in the radiative efficiency of lasers with a short (600 μm) cavity and to the change of their operation regime to the two-band lasing.**

Keywords: *semiconductor lasers, heterostructure, pulsed pumping, lasing spectrum.*

1. Introduction

High-power pulsed semiconductor lasers have a wide range of practical applications (free-space communications, metrology, materials processing, etc.). Recently, the fields of laser range finding and lidar complexes are extensively developed in order to plot 3D space images for driverless vehicles. Studies in this direction require lasers operating in a wide temperature range with minimal decrease in their efficiency. Previously, we have studied semiconductor lasers emitting in the spectral range 1000–1100 nm at liquid-nitrogen temperatures under ultrahigh pumping [1]. It was shown that, in a pulsed regime (pulse duration 100 ns, repetition rate 1 kHz), a decrease in temperature from 300 to 110 K makes it possible to increase the radiative efficiency in the range of high currents and, as a result, to increase the peak optical power from 58 to 90 W (for a pump current of 100 A). This increase in power at lower temperatures was related to a decrease in the concentration of excess charge carriers in the waveguide layers of the heterostructure. It was shown in experimental [2] and theoretical [3,4] works that the optical power of lasers emitting in the spectral range 1000–1100 nm considerably decreases with increasing internal optical losses, which is related to accumulation of excess charge carriers in waveguide layers. In addition, studies were performed on the influence of spatial hole burning [5] and gain saturation [6] on the differential efficiency of pulsed light–current characteristics (LCCs). On the other hand, operation of a laser at ultrahigh excitation levels is accompanied by changes in its spectral characteristics. Two-level lasing in the range of the LCC saturation was observed in [7,8]. Detailed studies of lasing dynamics showed that the laser wavelength switches during the laser pulse from the fundamental, long-wavelength line (corresponding to the 1e – 1h transition), to the short-wavelength line (corresponding to the 2e – 2h transitions). In this case, lasing can occur both simultaneously at two lines (mixed regime) and only at the short-wavelength line. Under the conditions when the distance between the lines reaches 70 nm, these lasing regimes complicate solving the range finding problems and make it necessary to use spectral filters to reduce the influence of extra light.

Note that the main attention in the previous experiments was given to the radiative characteristics of semiconductor lasers at ultrahigh excitation levels, while their operation in a pulsed pumping regime at high temperatures was not studied separately. In the present work, we study the radiative characteristics of semiconductor lasers under pulsed pumping at increased (up to 90 °C) temperatures and determine the factors affecting their radiative efficiency in the range of high temperatures at high injection currents.

2. Experimental samples

Experimental studies [9] showed that semiconductor lasers based on asymmetric heterostructures with a broad multimode waveguide and one quantum well have low optical losses and retain high radiative efficiency at room temperature. However, the low optical confinement factor in the active region leads to a strong temperature dependence of the threshold current [10]. In addition, according to calculations, there exists significant accumulation of excess electrons and holes in the p-region of the waveguide [4]. Because of this, in the present study we used an optimized heterostructure design for laser operation at high temperatures and high excitation levels.

The heterostructure included n-AlGaAs (x = 15%) and p-AlGaAs (x = 30%) wide-gap emitters and an AlGaAs (x = 10%) waveguide 1.05 μm thick on the n-emitter side. The waveguide layer on the p-emitter side was 0.64 μm thick and

P.S. Gavrina, A.A. Podoskin, D.A. Veselov, V.V. Shamakhov, S.O. Slipchenko, N.A. Pikhtin, P.S. Kop'ev Ioffe Institute, Russian Academy of Sciences, ul. Politekhnicheskaya 26, 194021 St. Petersburg, Russia; e-mail: podoskin@mail.ioffe.ru;
E.V. Fomin Elfolum Ltd, Politekhnicheskaya ul. 28, 194021 St. Petersburg, Russia

Received 5 November 2020; revision received 25 November 2020
Kvantovaya Elektronika **51** (2) 129–132 (2021)
Translated by M.N. Basieva

had a composition varying from AlGaAs (x = 10%) to AlGaAs (x = 30%). The active region included two InGaAs quantum wells with a thickness of 9 nm each. The use of two quantum wells allowed us to increase the optical confinement factor in the active region from 1% to 1.5%, while the gradient waveguide on the p-emitter side was intended to decrease the concentration of excess carriers at high pump currents. The developed heterostructure was grown by MOCVD. From this heterostructure, we fabricated stripe semiconductor lasers with the emitting aperture 100 μm wide and a cavity length L in the range of 600–2900 μm. The Fabry–Perot cavity faces were coated with antireflection [11] and reflection layers with reflection coefficients of 5% and 95%, respectively. The semiconductor laser crystals were mounted with the p-side down on copper heat sinks using indium solder.

3. Experimental results

The radiative characteristics were studied using a measuring setup including a pulsed pump current source (pulse duration 100 ns, pulse repetition rate 1 Hz, amplitude 0.5–123 A), a temperature stabilisation system to keep constant the required temperature in the range of 20–90 °C, a lens system for light focusing, a G8421 InGaAs photodiode (Hamamatsu) with a response time of 500 ps and a sensitivity variation not exceeding 20% in the spectral range 1010–1090 nm to estimate the optical pulse shape, an oscilloscope with a frequency band of 2 GHz, an Ophir 3A-P-FS-12 thermal sensor to record the average optical power in the range from 15 mW to 3 W, and an Advantest Q8384 spectrum analyser to measure the laser spectra.

Figure 1 shows the LCCs of semiconductor lasers with cavity lengths of 600, 1000, and 2900 μm obtained at temperatures T = 25 and 90 °C. One can see that the highest power (62 W at a current of 123 A) is demonstrated by the sample with a cavity length of 2900 μm. The maximum power at room temperature is limited by the growth of internal optical losses, which makes a noticeable contribution to the change of the LCC slope for currents exceeding 20 A. It is important to note that, at room temperature and currents of 0–50 A, a decrease in the cavity length from 2900 to 600 μm has no considerable effect on the LCC slope despite the fact that the increase in the internal optical losses related to accumulation of excess charge carriers in waveguide layers is stronger for lasers with L = 600 μm (current density for lasers with L = 600 μm is 4.8 times higher than for lasers with a cavity length of 2900 μm). This effect is explained by a smaller contribution of internal optical losses to the decrease of the differential efficiency η for lasers with higher output losses, which, in our case, are obtained due to a decrease in the cavity length [12].

An increase in temperature leads to a decrease in the differential efficiency. In this case, the slope of the initial LCC region decreases by 22% – 30% depending on the cavity length (see the inset in Fig. 1), and the maximum power for lasers with a cavity length of 2900 μm at T = 90 °C is 43 W at a pump current of 122 A. In addition, an increase in temperature to 90 °C noticeably changes the LCC character for lasers with short cavities in the range of high pump currents, which manifests itself in the appearance of kinks in the LCC. The shorter the laser cavity, the lower the current at which an LCC kink is observed. While the first kink for the sample with L = 600 μm appears even at 30 A, a kink for lasers with L = 1000 μm is observed at 40 A, and for lasers with L = 2900 μm there exists no kinks at all in the studied range of currents.

An increase in temperature most strongly affects the LCC shape of samples with a cavity length of 600 μm, because of which we will consider the specific features of their operation at different temperatures in more detail. Figure 2 presents the dependences of the average laser power measured by a thermal sensor on the pump current at temperatures of 25, 40, 60, and 90 °C. One can see that the LCC shape at low pump currents is close to linear at any temperature. An increase in current is accompanied by a noticeable decrease in the local differential efficiency η_{loc} (η_{loc} is determined as the derivative of the light–current function for a chosen current value). At a temperature of 90 °C and a current of ~40 A, η_{loc} is partially restored.

In addition, the samples wit L = 600 μm exhibit deformation of the optical pulse shape at high pump levels, and this deformation increases with increasing temperature. Figure 3 shows a series of typical pump current pulses with amplitudes

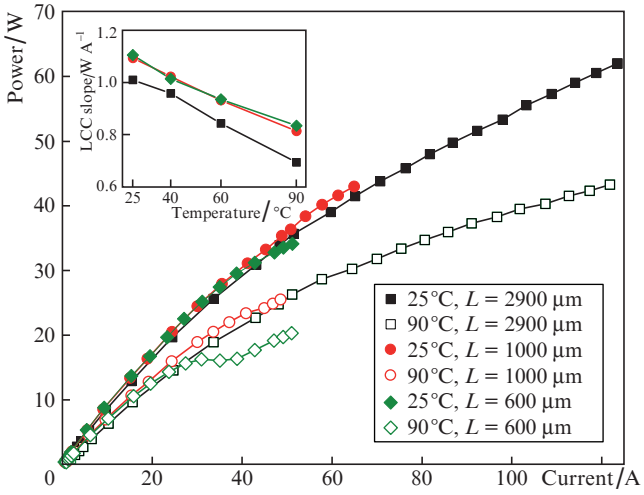

Figure 1. Light–current characteristics of semiconductor lasers with different cavity lengths pumped by current pulses (100 ns, 1 kHz) at temperatures of 25 and 90 °C. The inset shows the temperature dependence of the LCC slope in the initial region.

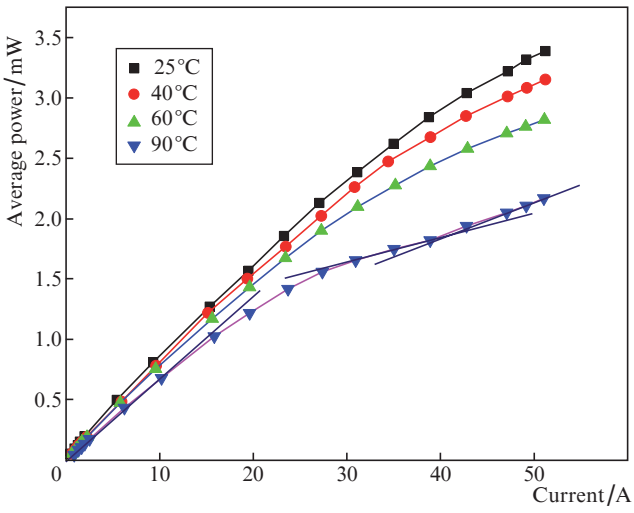

Figure 2. Dependences of the average power of a laser with a cavity length of 600 μm on the pump current at different temperatures.

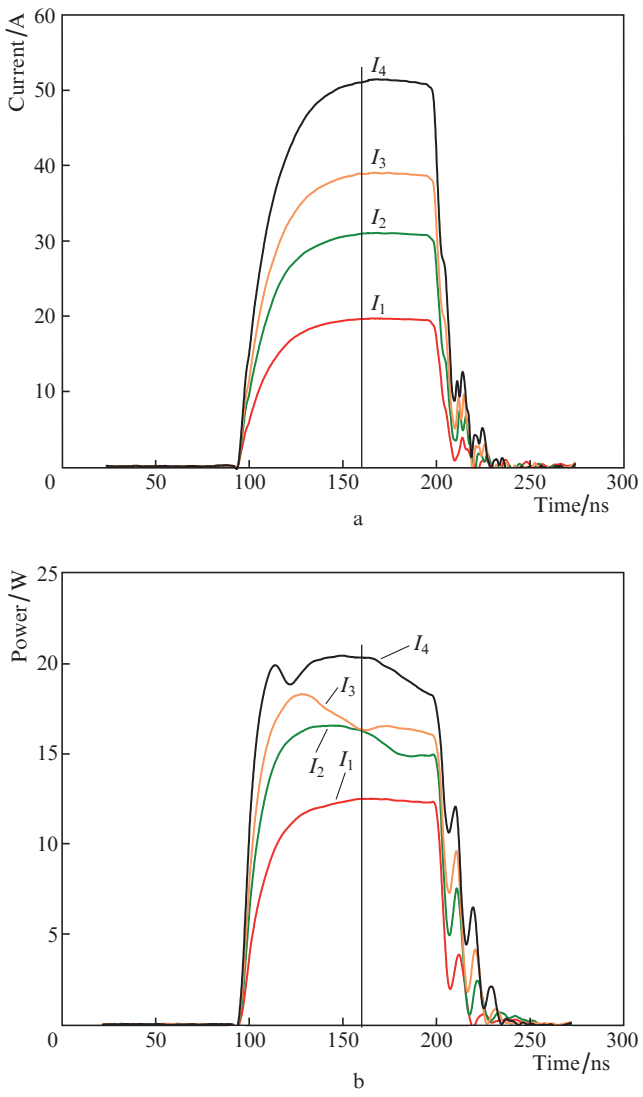

Figure 3. (a) Current and (b) optical pulses of a laser with a cavity length of 600 μm at a temperature of 90 °C and increasing pump currents $I_1 - I_4$. The vertical line corresponds to $t = 160$ ns.

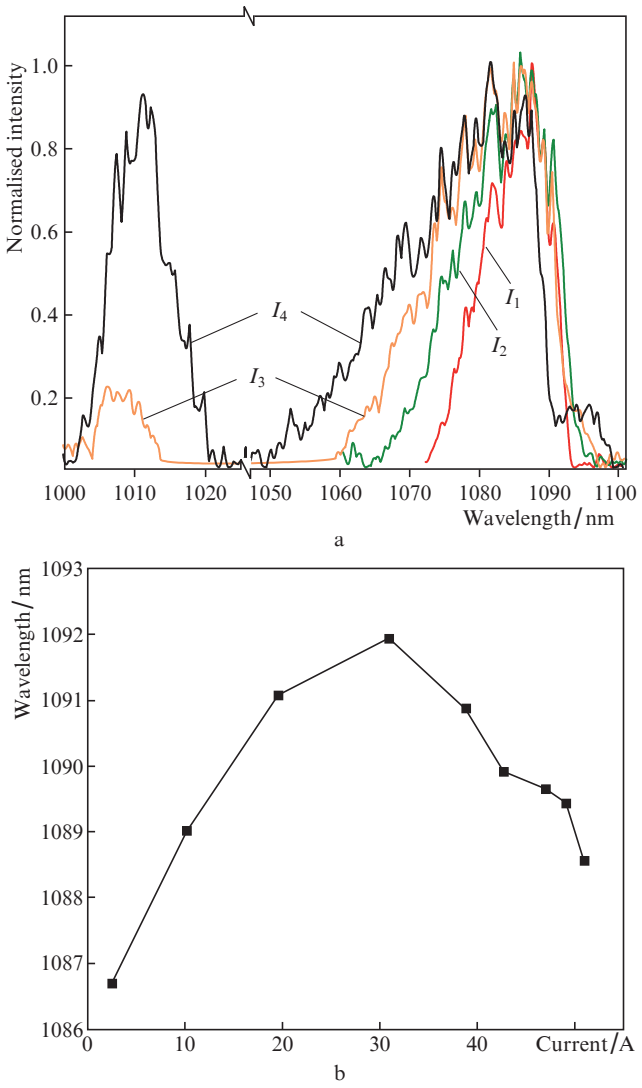

Figure 4. (a) Laser spectra recorded at increasing pump currents $I_1 - I_4$ and (b) dependence of the position of their long-wavelength edges at half maximum of normalised amplitude. The laser cavity length is 600 μm, the temperature is 90 °C.

increasing from I_1 to I_4 and the corresponding optical pulses at $T = 90$ °C. One can see that the shapes of the optical and electric signals well coincide at low currents (I_1). With increasing current, one observes deformation of the optical pulse shape, which begins from the end of the pulse and manifests itself in a gradual decrease in the optical power in the deformation region with respect to the level corresponding to the leading part of the pulse. Further increase in the current leads to even larger relative decrease in the power, and the beginning of the power dip shifts to the beginning of the pulse (currents I_2 and I_3 in Fig. 3). The optical power level in the dip is partially restored at currents exceeding 40 A, which corresponds to the region of partial recovery of the local differential efficiency (see Fig. 2). Deformation of the optical pulse is also observed in the case of samples with cavity lengths of 1000 and 2900 μm, but is considerably weaker than that for lasers with a length of 600 μm.

The vertical line in Fig. 3 indicates the time instant (t = 160 ns) corresponding to the maximum amplitude of the electric pulse at low currents, which was used for plotting the LCCs shown in Fig. 1. Note that the choice of another time instant causes no principal changes in the LCC shape.

Since lasing in the samples with a cavity length of 600 μm is accompanied by the appearance both of features in the optical pulse shape and of kinks in the LCCs, it is of interest to study their spectra at a temperature of 90 °C (Fig. 4). At currents of up to 20 A, one observes a typical shift of the long-wavelength edge of the spectrum to the red; the rate of this shift decreases at currents exceeding 20 A, and, beginning from 30 A, the long-wavelength edge shifts to the blue (Fig. 4b). The second line, which is shifted from the main line to shorter wavelengths by 70 nm, appears in the spectrum at a current of ~40 A (Fig. 4a). It is important to note that, at pump currents corresponding to the LCC range in which the local differential efficiency is partially recovered, the laser operates in the two-level regime. Thus, the appearance of the second laser line does not cause a decrease in the local differential efficiency. Note that the emission spectra of lasers with a cavity length of 600 μm at temperatures of 25, 40, and 60 °C do not have the second laser line, and the shift the long-wavelength edge to shorter wavelengths does not occur.

4. Conclusions

The performed investigations showed that the proposed heterostructure design makes it possible to achieve efficient operation of semiconductor lasers at temperatures increased to 90 °C. In addition, the use of short cavity lengths (600 μm) does not cause a decrease in the peak power at currents of up to 50 A and a temperature of 25 °C. However, a significant increase in the working temperature (up to 90 °C) of these lasers is accompanied by a decrease in the radiative efficiency at high pump currents. One of the reasons for this effect can be insufficient gain (gain saturation), which is a result of two-level lasing. The use of lower threshold concentrations of excess carriers and lower material gains can be considered as a method of solving this problem, which will be the subject of subsequent publications.

Acknowledgements. This work was supported by the Russian Science Foundation (Project No. 19-79-30072).

References

1. Veselov D.A., Shashkin I.S., Bobretsova Yu.K., Bakhvalov K.V., Lyutetskii A.V., Kapitonov V.A., Pikhtin N.A., Slipchenko S.O., Sokolova Z.N., Tarasov I.S. *Fiz. Tekh. Poluprodn.*, **50** (10), 1414 (2016).
2. Veselov D.A., Bobretsova Y.K., Leshko A.Y., Shamakhov V.V., Slipchenko S.O., Pikhtin N.A. *J. Appl. Phys.*, **126**, 213107 (2019).
3. Piprek J. *Opt. Quantum Electron.*, **51**, 1 (2019).
4. Soboleva O.S., Zolotarev V.V., Golovin V.S., Slipchenko S.O., Pikhtin N.A. *IEEE Trans. Electron Devices*, **67** (11), 4977 (2020).
5. Wenzel H., Crump P., Pietrzak A., Roder C., Wang X., Erbert G. *Opt. Quantum Electron.*, **41** (9), 645 (2009).
6. Knigge A., Klehr A., Wenzel H., Zeghuzi A., Fricke J., Maaßdorf A., Liero A., Tränkle G. *Phys. Status Solidi A*, **215** (8), 1700439 (2018).
7. Veselov D.A., Ayusheva K.R., Pikhtin N.A., Lyutetskiy A.V., Slipchenko S.O., Tarasov I.S. *J. Appl. Phys.*, **121**, 163101 (2017).
8. Sokolovskii G.S., Vinokurov D.A., Deryagin A.G., Dyudelev V.V., Kuchinskii V.I., Losev S.N., Lyutetskii A.V., Pikhtin N.A., Slipchenko S.O., Sokolova Z.N., Tarasov I.S. *Tech. Phys. Lett.*, **34** (8), 708 (2020) [*Pis'ma Zh. Tekh. Fiz.*, **34** (16), 58 (2008)].
9. Slipchenko S.O., Vinokurov D.A., Pikhtin N.A., Sokolova Z.N., Stankevich A.L., Tarasov I.S., Alferov Zh.I. *Fiz. Tekh. Poluprovodn.*, **38**, 1477 (2004).
10. Slipchenko S.O., Shashkin I.S., Vavilova L.S., Vinokurov D.A., Lyutetskii A.V., Pikhtin N.A., Podoskin A.A., Stankevich A.L., Fetisova N.V., Tarasov I.S. *Fiz. Tekhn. Polupr.*, **44**, 688 (2010).
11. Fomin E.V., Bondarev A.D., Soshnikov I.P., Bercu N.B., Giraudet L., Molinari M., Maurer T., Pikhtin N.A. *Tech. Phys. Lett.*, **46** (3), 268 (2020) [*Pis'ma Zh. Tekh. Fiz.*, **46** (6), 16 (2020)].
12. Veselov D.A., Pikhtin N.A., Lyutetskii A.V., Nikolaev D.N., Slipchenko S.O., Sokolova Z.N., Shamakhov V.V., Shashkin I.S., Kapitonov V.A., Tarasov I.S. *Quantum Electron.*, **45** (7), 597 (2015) [*Kvantovaya Elektron.*, **45** (7), 597 (2015)].